Medicine®

OPEN

Time resolved DCE-MRI of the kidneys
Evaluation of the renal vasculatures and tumors using F-DISCO with and without compressed sensing in normal and wide-bore 3T systems

Takahiro Yamada, MD[a] [ID], Takayuki Masui, MD, PhD[a],*, Masako Sasaki, MD[a], Motoyuki Katayama, MD, PhD[a], Yuji Iwadate, MS[b], Naoyuki Takei, MS[b], Mitsuharu Miyoshi, MS[b]

Abstract

Dynamic contrast-enhanced MR imaging (DCE-MRI) has been widely used for the evaluation of renal arteries. This method is also useful for tumor and renal parenchyma characterization. The very fast MRI may provide stable and precise information regarding vasculature and soft tissues. The purpose of this study was to evaluate the ability of DCE-MRI to assess renal vasculatures and tumor perfusions using Differential subsampling with Cartesian ordering with spectrally selected inversion recovery with adiabatic pulses (F-DISCO) with and without compressed sensing (CS) in normal and wide-bore 3T systems.

Fifty-one patients who underwent DCE-MRI using F-DISCO with or without CS for evaluation of renal or adrenal regions were included. Image quality, artifacts, fat saturation, and selective visual recognition of renal vasculatures were assessed by using a 5-point scale. Tumor recognition was verified by using a 5-point scale of confidence level. Signal intensities of each structure were also measured.

In all cases, the temporal resolution of each phase for DCE-MRI was 1.9 to 2.0 seconds. Image quality, artifacts, fat saturation, and selective visual recognition of vasculatures were all acceptable (mean score 4.2–4.9). The selective visualization of renal arteries and veins was successfully accomplished (mean score 4.0–4.9). Contrast media perfusion for renal vasculature, renal parenchyma, and tumors was also recognized.

DCE-MRI for the evaluation of renal vasculatures and tumors using F-DISCO with or without CS can be performed with high temporal and spatial resolutions in normal and wide-bore 3T systems. This information can be obtained in a stable fashion throughout the dynamic contrast study. CS can additionally provide benefits that the total imaging time may be shorter than without CS.

Abbreviation: CS = compressed sensing, CTA = computed tomography angiography, DCE-MRA = dynamic contrast-enhanced magnetic resonance angiography, DCE-MRI = dynamic contrast-enhanced magnetic resonance imaging, DISCO = Differential subsampling with Cartesian ordering, F-DISCO = Differential subsampling with Cartesian ordering with a fat suppression pulse of spectrally selected adiabatic inversion recovery, FSPGR = fast spoiled gradient echo recalled acquisition in the steady state, ROI = regions of interest, SI = signal intensity, Spec IR = spectrally selected inversion recovery, TR = repetition time.

Keywords: compressed sensing, contrast-enhanced MRI, fast imaging, fat saturation, view-sharing

1. Introduction

Dynamic contrast-enhanced MR angiography (DCE-MRA) with gadolinium-based contrast media and CT angiography (CTA) with iodine contrast media have been widely used in body imaging.[1–3] Compared with CTA, one of the advantages of DCE-MRA is that multiple acquisitions of MR images can be performed without exposure to x-ray radiation. For selective visualization of the renal arteries and veins, fast dynamic contrast imaging techniques are necessary, and various techniques

have been introduced.[4,5] Subsequently, this has led to the wide use of centric k-space data sampling that can efficiently utilize data of k-space center to facilitate the desired contrast and data of k-space periphery to enable anatomy delineation.[4,5] Even when the imaging time is longer, centric k-space data sampling allows the effective delineation of the renal arteries in a single phase without any overlap between renal veins and parenchyma.[4,5] However, longer imaging times, approximately 20 to 25 seconds per phase, may lead to a loss of useful information regarding renal parenchyma and tumor perfusion in dynamic

contrast-enhanced MR imaging (DCE-MRI). This is because a considerable acquisition time needs to be required to sample k-space periphery data for anatomy delineation compared to contrast resolutions. For detection and characterization of renal tumors, several previous studies have reported that DCE-MRI can provide useful information.[6–8] Focusing on tissue perfusions, multiple phases with short imaging times per phase can provide better tissue contrast perfusions without losing useful information and vascular anatomy visualization.[9]

To accelerate temporal resolution in DCE-MRI, Differential subsampling with Cartesian ordering (DISCO) can be employed. This method is a DCE-MRI technique that is based on a 3D fast spoiled gradient echo recalled acquisition in the steady state (FSPGR) sequence with a view-sharing technique.[10] View-sharing technique in DISCO may cause some blurring effects on the anatomical delineation over several phases when motions occur during data acquisitions and may induce contaminations of contrast when dynamic contrast study is performed. Shorter imaging for 1 phase will minimize these undesirable effects. Especially on a wide-bore system longer imaging time may be required since lower slew rate is expected compared with on a normal-bore system. Fat signal suppression for T1WI may be important to enhance contrast resolution. However, uniform fat suppression at higher field strengths has been one of the major obstacles to overcome because of B_0 and B_1 inhomogeneity.[11] In contrast, 2-point Dixon fat–water separation can offer homogenous fat suppression although this method requires 2 echoes, and this is the method applied to DISCO.[10] The Dixon water–fat separation method of bipolar acquisition increases the demands on gradient performance.[12] This may in turn induce a prominent prolongation of repetition time (TR) in wide-bore 3T systems compared with normal-bore 3T systems. Another approach to facilitate fat signal suppression is to use the spectrally selected inversion recovery (Spec IR) technique. The efficient use of an adiabatic pulse as Spec IR for fat signal suppression allows the acquisition of images with higher temporal resolution compared with using Dixon water–fat separation. This is because the use of a single short echo time induces a shorter TR instead of dual-echo acquisitions. Using DISCO with a fat suppression pulse of spectrally selected adiabatic inversion recovery (F-DISCO) may reduce the gradient performance difference between wide-bore and normal-bore 3T systems, and competitive imaging time for the dynamic contrast study can be accomplished in both 3T systems. Another strategy to accelerate data acquisition involves compressed sensing (CS), a technique based on the acquisition of randomly undersampled k-space to accelerate MR imaging.[13]

Accordingly, the purpose of this study was to evaluate the abilities of DCE-MRI to assess renal vasculatures and tissue perfusions, including tumors, using F-DISCO with and without CS in normal and wide-bore 3T systems.

2. Materials and Methods

2.1. Study population

Our study was approved by the institutional review board in our hospital, and written informed consent was obtained from all patients included. MR imaging was performed in 3.0T MRI scanners with a normal-bore size (Discovery MRI 750[MR750], General Electronic [GE] Healthcare, Milwaukee, WI) or with a wide-bore size (Discovery MRI 750W(MR750W), GE Healthcare]. Between July 2017 and April 2020, 54 patients who underwent DCE-MRI for the evaluation of renal or adrenal lesion were included. The subjects were divided into 4 groups: F-DISCO with CS on MR750, F-DISCO with CS on MR750W, F-DISCO without CS on MR750, and F-DISCO without CS on MR750W (Fig. 1). Out of the 54 patients included, 32 patients underwent DCE-MRI using F-DISCO with CS between May 2019 and April 2020, and 22 patients underwent DCE-MRI using F-DISCO without CS between July 2017 and October

2018. Eventually, 3 patients were excluded from this study. One patient in F-DSICO with CS was excluded because it was not feasible to evaluate the right renal vein because of the extent of tumor invasion. In addition, 2 patients in F-DISCO without CS were excluded, 1 with atrophic right kidney and right renal artery and 1 because of incomplete study data.

Resultantly, 16 patients underwent DCE-MRI using F-DISCO with CS on MR750, 15 patients using F-DISCO with CS on MR750W, 13 patients using F-DISCO without CS on MR750, and 7 patients using F-DISCO without CS on MR750W.

Eighteen patients were diagnosed with renal tumors, and 10 patients with adrenal tumors. Among these 28 patients, 10 patients underwent surgical operations, and 6 patients were examined by CT or MRI at 6 to 12 months after the initial examinations to confirm no changes in tumor size and characteristics. Four patients had already undergone CT or MRI 6 to 12 months before the current examination, which also confirmed no changes in tumor size. One patient underwent biopsy, which, in turn, indicated the manifestation of a renal cell carcinoma, whereas 1 patient with tuberous sclerosis had a renal angiomyolipoma. One patient suspected renal carcinoma from MRI was transferred other hospital. There were 5 patients for whom no follow-up imaging was performed and who were clinically diagnosed with angiomyolipomas (in 2 patients), cortical adenoma (in 2 patients), and pyelonephritis.

2.2. MR imaging techniques

Data acquisition was accomplished by DISCO, which is a 4D MRI technique with high-spatial–temporal resolution for accelerated dynamic imaging with pseudo-random segmentations in k-space acquisition. The segmented k-space has annular regions that consist of a central region A that is fully sampled and multiple outer regions Bi ($i = 1 – N$, where N is the number of B regions) that are subsampled. The outer region has different subsampling patterns that provide a pseudo-random distribution of k-space on a Cartesian grid. The fat suppression technique uses chemically selective fat suppression with adiabatic inversion pulse that is applied to segmented k-space views containing points from both the central A region and the outer Bi regions.[14] For the acquisition of combined CS and parallel images, randomly undersampled k-space points in ky–kz space are prepared beforehand, and the DISCO sampling pattern is applied to the k-space.[15] After acquisition, each temporal phase dataset is composed of an A region and multiple Bi regions from neighbor view-sharing. Consequently, randomly undersampled data on ky–kz space with a Gaussian pattern for CS are reconstructed using L1-norm minimization of total variation forcing sparsity in an iterative manner to recover uniform k-space in the parallel image domain. Finally, data-driven parallel imaging with auto-calibration signal points generates the complete k-space.[16]

2.3. MR imaging protocol

Breath-hold (BH) dynamic contrast MR imaging was performed in MR750 or 750W 3T systems with 32-channel phased-array coils in a coronal plane using F-DISCO with or without CS. The following parameters were used for the group of F-DISCO without CS: ARC factor 2 × 1.8, TR 4 ms, matrix 256 × 224, FOV350 or 380 mm, slice thickness 3 or 4 mm with Spec IR using adiabatic pulses. Slab thickness was 184 to 334 mm (average 251 mm) for the group of F-DISCO with CS and that was 204 to 368 mm (average 240 mm) for the group of F-DISCO without CS.

Resultantly, similar temporal resolutions per phase were settled. For DISCO, each temporal phase dataset was composed of 1 A region and 3 Bi regions from neighbor view-sharing. The temporal resolution per phase was 1.9 to 2.0 seconds. For the group of F-DSICO with CS, the parameters were identical apart from

the use of CS corresponding to a factor of 1.4, and the temporal resolution per phase was 1.5 to 2.1 seconds. Consecutive 20 to 30 phases were obtained during BH as long as possible and were followed by quiet free breathing. And additional 2 phases were obtained 60 and 90 seconds after injection of Gd-chelate (injection of 0.1 mmol/kg gadobutrol at 1.0 mL/s followed by saline injection at 3.0 mL/s), respectively. Delayed phase was obtained during BH using liver imaging with volume acceleration-flexible 120 to 180 seconds after injection of contrast medium. The difference in total imaging time between using and not using CS was approximately 2 to 3 seconds. Initial imaging started 5 seconds after injection of Gd-chelate.

2.4. Imaging analysis

2.4.1. Subjective assessment. Source images and partial maximum intensity projection (MIP) images for MR angiography were independently reviewed by 2 radiologists with 5 and 14 years of experience. Partial MIP images were reconstructed on a workstation (Advantage window suite: AW Suite, GE Healthcare). Among dynamic contrast images, the first phase for contrast enhancement was determined, in which contrast enhancement of both the abdominal aorta and renal arteries was initially recognized. When the discrepancy occurred for recognitions, consensus was obtained between 2 radiologists. Subjectively, image quality, motion artifact, blurring artifact, and fat signal suppression homogeneity of retroperitoneal fat tissue were evaluated in the first phase using a 5-point scale (1 representing "undiagnostic, or inhomogeneous fat signal suppression" to 5 representing "excellent, no artifacts, or homogenous suppression"). Images scored above 3 points were regarded clinically diagnostic. Recognitions of the aorta were performed at 2 levels: upper (from the diaphragm to the renal arteries) and lower (from the renal arteries to the aortic bifurcation). Renal arteries at 4 segments (the proximal half and distal half of the main renal and the first- and second-order branches) were ranked using a 5-point scale (1 representing "not recognized" to 5

Table 1

Imaging time for 1 phase with each sequence.

	Imaging time
MR750 w CS (n = 16)	1.85 ± 0.17*
MR750 w/o CS (n = 13)	1.99 ± 0.03
MR750W w CS (n = 15)	2.03 ± 0.07
MR750W w/o CS (n = 7)	1.99 ± 0.03

The numbers indicate seconds ± standard deviation.
CS = compressed sensing.
*Significant difference against MR750 w/o CS (P = .007).

Table 2

Average score of image quality, artifacts, and degree of fat suppression.

	Image quality	Motion	Blurring	Fat suppression
MR750 w CS (n = 16)	4.4	4.9	4.4	4.5
MR750 w/o CS (n = 13)	4.6	4.9	4.4	4.4
MR750W w CS (n = 15)	4.2	4.9	4.2	4.2
MR750W w/o CS (n = 7)	4.8	4.8	4.4	4.4

MR750 w CS and MR750 w/o CS indicate 3T magnet MR750 with and without compressed sensing, respectively. MR750W indicates a 3T magnet with a wide bore. Motion and blurring indicate motion and blurring artifacts, respectively. Fat suppression indicates homogenous fat signal suppression. n indicates the total number of patients.
CS = compressed sensing.

Table 3

Average recognition score of aorta and renal arteries.

	U aorta	L aorta	Pro RRA	Dis RRA	1st RRA	2nd RRA	pro LRA	dis LRA	1st LRA	2nd LRA
MR750 w CS	4.7	4.7	4.4	4.3	4.6	4.3	4.9	4.8	4.9	4.5
MR750 w/o CS	4.5	4.7	4.5	4.7	4.5	4.0	4.7	4.7	4.5	4.2
MR750W w CS	4.5	4.4	4.2	4.3	4.6	4.0	4.7	4.5	4.7	4.3
MR750W w/o CS	4.5	4.6	4.6	4.6	4.6	4.1	4.9	4.9	4.7	4.2

MR750 w CS and MR750 w/o CS indicate 3T magnet MR750 with and without compressed sensing, respectively. MR750W indicates a 3T magnet with a wide bore. U aorta and L aorta indicate upper aorta and lower aorta, respectively. RRA and LRA indicate right renal artery and left renal artery, respectively. Pro and dis indicate proximal and distal, respectively. 1st and 2nd indicate the branch of each renal artery.
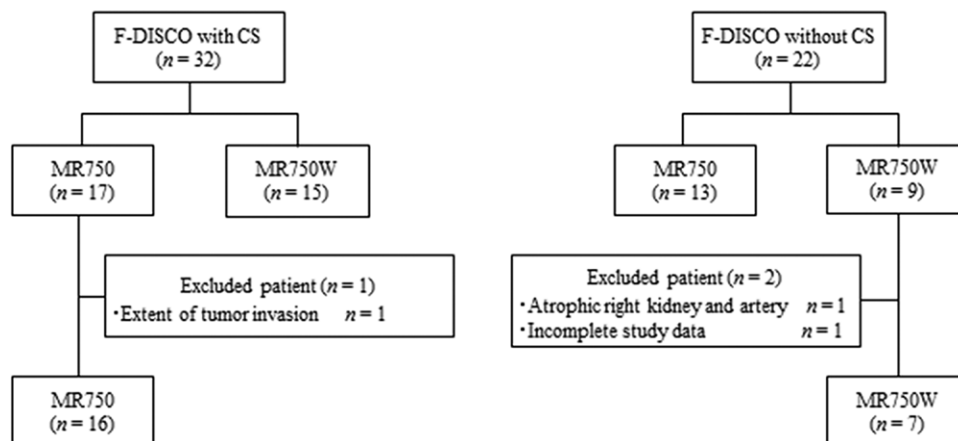CS = compressed sensing.

Figure 1. Flowchart for the study population.

representing "well recognized") on first phase images. The number of phases without any overlap between the renal artery and renal vein were then evaluated. Tumor recognition was assessed using a 5-point scale confidence level (1 representing "not recognized" to 5 representing "clearly recognized") for the kidneys or adrenals. Tumors were defined as hypervascular when they were enhanced more than the surrounding parenchyma in the kidneys or adrenal glands, whereas tumors were defined as hypovascular when they were less enhanced than the surrounded soft tissues in all the dynamic contrast phases.

2.4.2. Objective assessment. One of the authors performed the following objective evaluations. The regions of interest (ROIs) with a size larger than 4 mm² were placed on the aorta, the renal arteries and veins, the renal medullas and cortexes, and the psoas muscles in the first 8 phases of dynamic contrast studies. Subsequently, their signal intensities (SIs) were measured. Identical ROIs placed before the acquisition of the first phases of the dynamic contrast study and SIs were also measured. SI ratio was calculated by dividing the SI of each ROI by the SI of the iliopsoas muscle. Time intensity curves were also generated.

Table 4

Selective visualization of renal arteries without overlap of the renal veins on each magnet with and without compressed sensing.

Phase	MR750 w CS (n = 16)	MR750 w/o CS (n = 13)	MR750W w CS (n = 15)	MR750W w/o CS (n = 7)
1ph	16 (100)	13 (100)	15 (100)	7 (100)
2ph	16 (100)	13 (100)	15 (100)	7 (100)
3ph	16 (100)	13 (100)	15 (100)	7 (100)
4ph	14 (87.5)	8 (61.5)	10 (66.7)	4 (57.1)
5ph	5 (31.2)	4 (30.8)	5 (33.3)	4 (57.1)
6ph	0 (0)	2 (15.4)	0 (0)	3 (42.9)
7ph	0 (0)	0 (0)	0 (0)	0 (0)

MR750 w CS and MR750 w/o CS indicate 3T magnet MR750 with and without compressed sensing, respectively. MR750W indicates a 3T magnet with a wide bore. Numbers indicate the number of cases. Numbers in parentheses indicate percentage of the cases. n indicates the total number of patients.
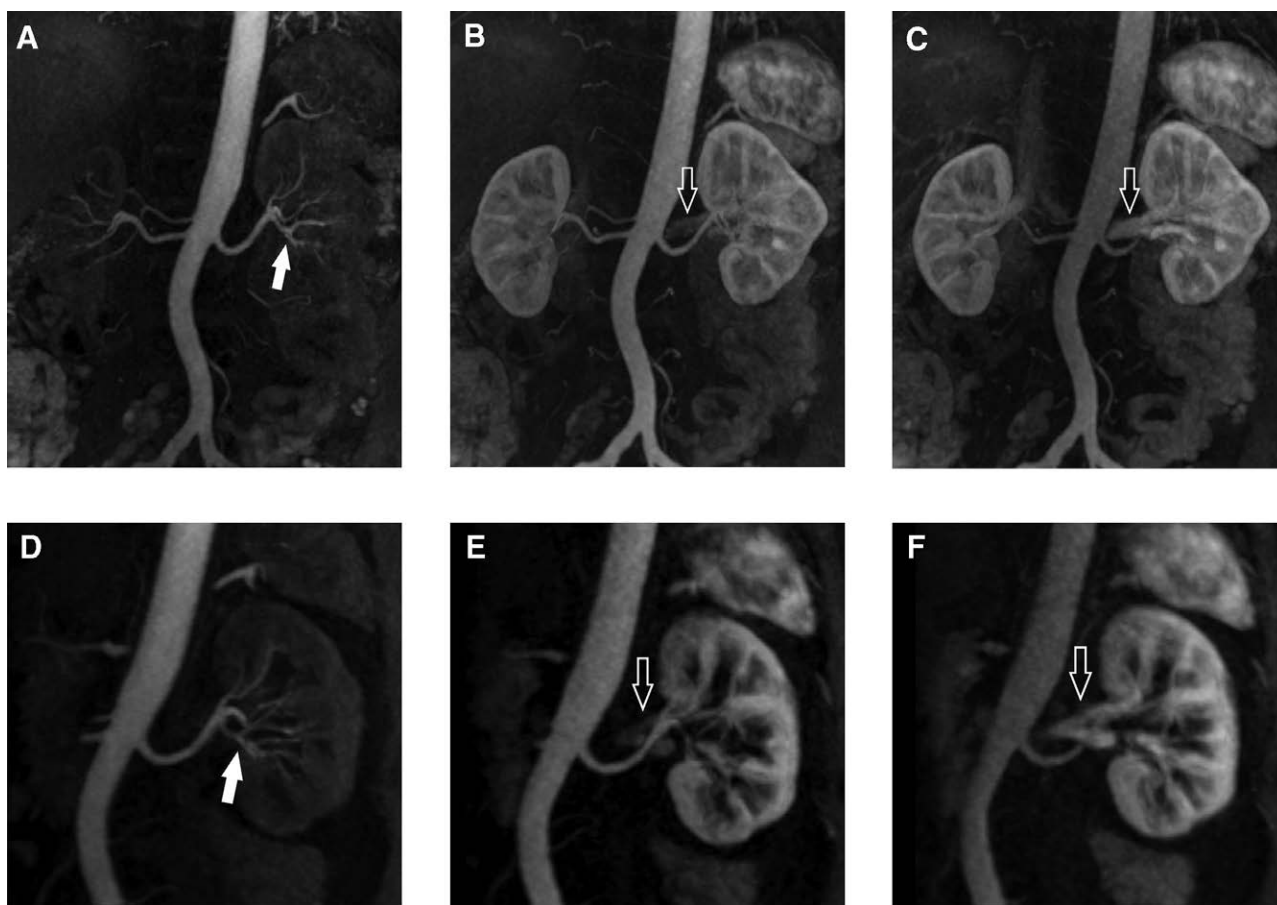CS = compressed sensing.

Figure 2. A 58-year-old woman who underwent DCE-MRI using F-DISCO without CS on 750W for renal regions. (A–C) MIP images generated from data covering the entire region in each phase. (D–F) Partial MIP images generated from selected fewer volumes for left kidney in each phase. (A and D) In the first phase, the aorta and renal arteries (arrows) were selectively visualized without overlaps of renal veins or soft tissues. (B and E) In the fifth phase, the left renal vein (blank arrow) was slightly enhanced as the renal parenchyma. (C and F) In the seventh phase, renal arteries and veins (blank arrows) overlapped. DCE-MRI = dynamic contrast-enhanced magnetic resonance imaging, F-DISCO = Differential subsampling with Cartesian ordering with a fat suppression pulse of spectrally selected adiabatic inversion recovery, MIP = maximum intensity projection.
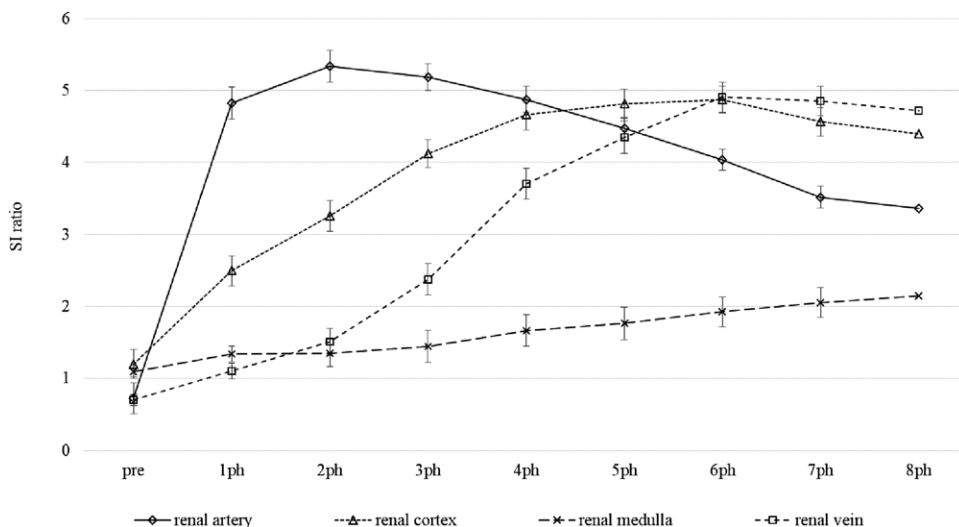
Figure 3. Time intensity curves of the left renal vasculatures and parenchyma after injection of contrast medium. The plotted values represent the mean contrast ratio ± standard error. Pre indicates initial phase after injection of contrast medium. Ph means phase.

2.5. Statistical analysis

All statistical analyses were performed using the EZR software (version 1.54, Saitama Medical Center, Jichi Medical University).

Sample size calculation was performed using the EZR software with estimated standard deviation and mean difference in average among groups.

Student t tests were used for the evaluation of each feature among the groups using pooled data. P value for significance was set to <.05. Boneferroni correction was applied.

SIs of the renal arteries and veins in the dynamic phases were compared using a 1-way ANOVA. P values less than .05 was considered significant.

3. Results

3.1. Imaging time

The average imaging time per phase was 1.85 and 1.99 seconds for F-DISCO with and without CS on MR750, respectively, and 2.03 and 1.99 seconds for F-DISCO with and without CS on MR750W, respectively. A significant difference was found between images with and without CS on MR750 (P = .007) (Table 1). Without CS, imaging time increased 1.85 to 2.51 on MR750 and 2.03 to 2.37 on MR750W for the groups of F-DISCO with CS. CS could accelerate the imaging speed, and the total imaging time with CS was approximately 10 seconds shorter than without the CS technique.

3.2. Result of subjective assessment

All images acquired from the 51 patients included in this study were diagnostic, and image quality and homogeneity of fat suppression were well observed, whereas motion and blurring artifacts were less recognized (Table 2).

All structures, including the aorta above and below the renal arteries, proximal to distal renal arteries, renal veins, renal cortex and medulla, and adrenals were well recognized (Table 3). Recognition of the upper- and lower-level aorta, renal medulla, and cortex were not significantly different among the 4 groups.

In all patients, the renal arteries and renal veins on the left side were separately visualized from the first to third phase, without any vasculature overlaps (Table 4, Fig. 2). Even in the fourth phase, there was no vasculature overlap recognized in the majority of our patients (Table 4).

3.3. Result of objective assessment

Changes in mean SIs in each anatomical structure with time was demonstrated in dynamic contrast studies. SIs on the left side was shown in Figure 3 as a representative because SIs on both sides were almost same profile. The SI peak of the renal arteries was observed in the second phase. There were significant differences in SIs between renal arteries and veins throughout the second to fourth phase. The average SI ratio of renal arteries/veins was 4.34 and 3.85 on MR750 with and without CS, respectively, and 3.33 and 3.40 on MR750W with and without CS on the right side of the first phase, respectively. In contrast, when the left side was investigated, these values changed to 5.04 and 4.46 on MR750 with and without CS, respectively, and 4.03 and 3.57 on MR750W with and without CS, respectively. There was no significant difference between the phase for the peak SIs of the renal arteries and the numbers of phases for the recognition of no overlap of the renal arteries and veins.

3.4. Evaluation of tumors

Both readers could detect all tumors in adrenal glands and kidneys, and they matched the tumor character, hypervascular or hypovascular, in all cases. Hypervascular tumors were detected in the adrenal glands of 10 patients, whereas 9 hypervascular tumors were identified in the kidneys (Table 5, Fig. 4). In the representative case of the hypervascular renal tumor, that is, clear cell cancer, DCE-MRI showed the early strong enhancement of the tumor, compared with the renal cortex and medulla, followed by the wash-out of the contrast medium (Fig. 5). In the representative case of the hypovascular renal tumor, that is, angiomyolipoma, DCE-MRI revealed that the tumor was less enhanced than the renal cortex (Figs. 6 and 7).

Table 5

Confidence levels of renal and adrenal tumors.

	Renal hypervascular tumor (n = 9)	Renal hypovascular umor (n = 9)	Adrenal tumor (n = 10)
Reader 1	4.8	4.4	3.7
Reader 2	4.7	4.1	3.3

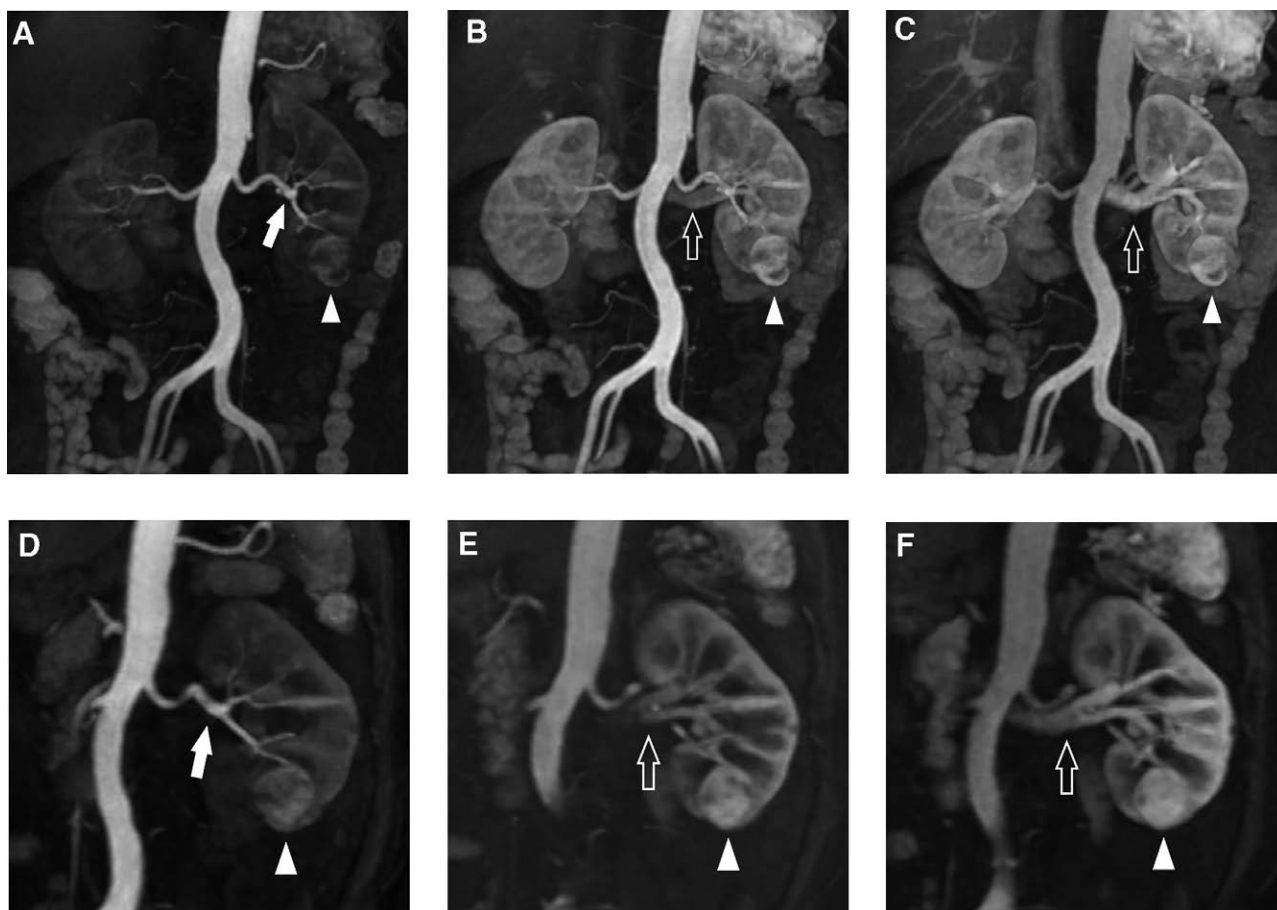n indicates a total number of patients.

Figure 4. A 61-year-old woman with renal carcinoma on the lower pole of the left kidney who underwent DCE-MRI using F-DISCO with CS on MR750. (A–C) MIP images generated from data covering the entire region in each phase. (D–F) Partial MIP images generated from the selected volumes for the left kidney in each phase. (A and D) In the first phase, the renal arteries (arrows) were well recognized without overlap of renal veins or soft tissues, and the tumor (arrow head) was well enhanced and demarcated. (B and E) In the fourth phase, the left renal vein (blank arrow) was slightly enhanced as the renal parenchyma. The tumor (arrow head) was well enhanced. (C and F) In the seventh phase, the enhanced renal veins (blank arrow) obscured the renal arteries. The tumor (arrow head) was well enhanced. DCE-MRI = dynamic contrast-enhanced magnetic resonance imaging, F-DISCO = Differential subsampling with Cartesian ordering with a fat suppression pulse of spectrally selected adiabatic inversion recovery, MIP = maximum intensity projection.
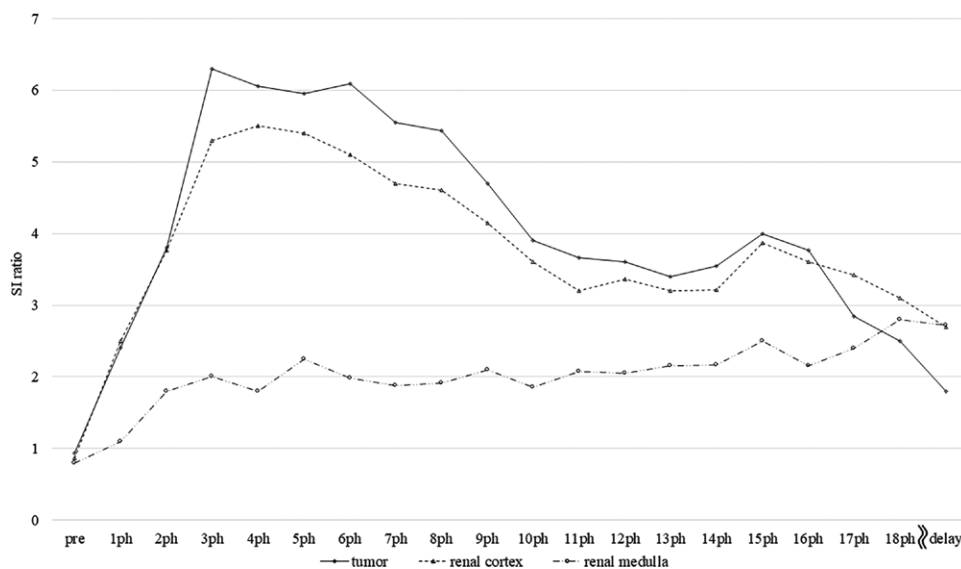

Figure 5. A 61-year-old woman, same patient as in Figure 4. Time intensity curves of the left renal tumor and parenchyma after injection of contrast medium. The plotted values are SI ratio calculated by dividing the SI of each ROI by the SI of the iliopsoas muscle. Pre indicates initial phase after injection of contrast medium. Ph means phase. Delay indicates delayed phase 120 to 180 seconds after injection of contrast medium. The imaging time per phase was 1.70 seconds. ROI = regions of interest, SI = signal intensity.

4. Discussion

Our current study demonstrates that DCE-MR using F-DISCO-based sequences in normal and wide-bore 3T scanners could provide efficient anatomical information of renal arteries and veins as well as tissue perfusions for kidneys, adrenals, and their tumors, with high temporal and spatial resolutions throughout dynamic contrast studies. This information can be obtained in a stable fashion throughout each dynamic contrast study. Without CS technique, selective visualization of the renal artery and vein can be performed; however, CS can additionally provide benefits that the total imaging time may be shorter approximately 10 seconds than without CS.

Several papers have reported the usefulness of DISCO in dynamic contrast imaging, which is based on the 2-point Dixon fast 3D FSPGR technique that, in turn, generates water-only, fat-only, in-phase, and out-of-phase images. This technique provides excellent homogeneous fat suppression over the entire field of view with water images and accelerates the imaging speed by using a 2D self-calibrated parallel imaging, and view-sharing techniques.[10,17,18] However, the original DISCO requires dual-echo acquisition, and the imaging time on a wide-bore 3T magnet is significantly longer than that of a normal-bore 3T owing to gradient coil performance limitations (In internal data, TR approximately increases from 2.4 ms on a normal-bore 3T to 3.2 ms on a wide-bore 3T). This facilitates lower temporal or spatial resolutions in dynamic MRI, and the resultant blurs pertaining to the delineation of each structure in the dynamic phase in a wide-bore scanner were expected to be inferior compared to those in the normal-bore scanner. The previous paper had reported that 4 to 5 seconds' temporal resolution with DISCO could be accomplished with a normal-bore 3T.[10] On a wide-bore 3T, it might be theoretically prolonged to 5.3 to 6.7 seconds. Because of the fast venous return of renal veins, overlap of the renal artery and vein may be expected. The currently used F-DISCO is based on 3D FSPGR with a single-echo acquisition. Thus, shorter TR can be applied, and the overall acquisition time for each dynamic phase with F-DISCO was significantly shorter compared with that using the original DISCO. As a result, temporal and spatial resolutions for an MR750 with a normal-bore 3T magnet and an MR750W with a wide-bore 3T magnet were almost competitive. We could set the imaging time for each phase to be shorter than 2 seconds in both 3T magnets, and competitive image quality for each dynamic contrast phase could be obtained in both MR750 and MR750W magnets.

For fat signal suppression, Spec IR can be applied together with adiabatic pulses. Fat saturation with adiabatic pulses is
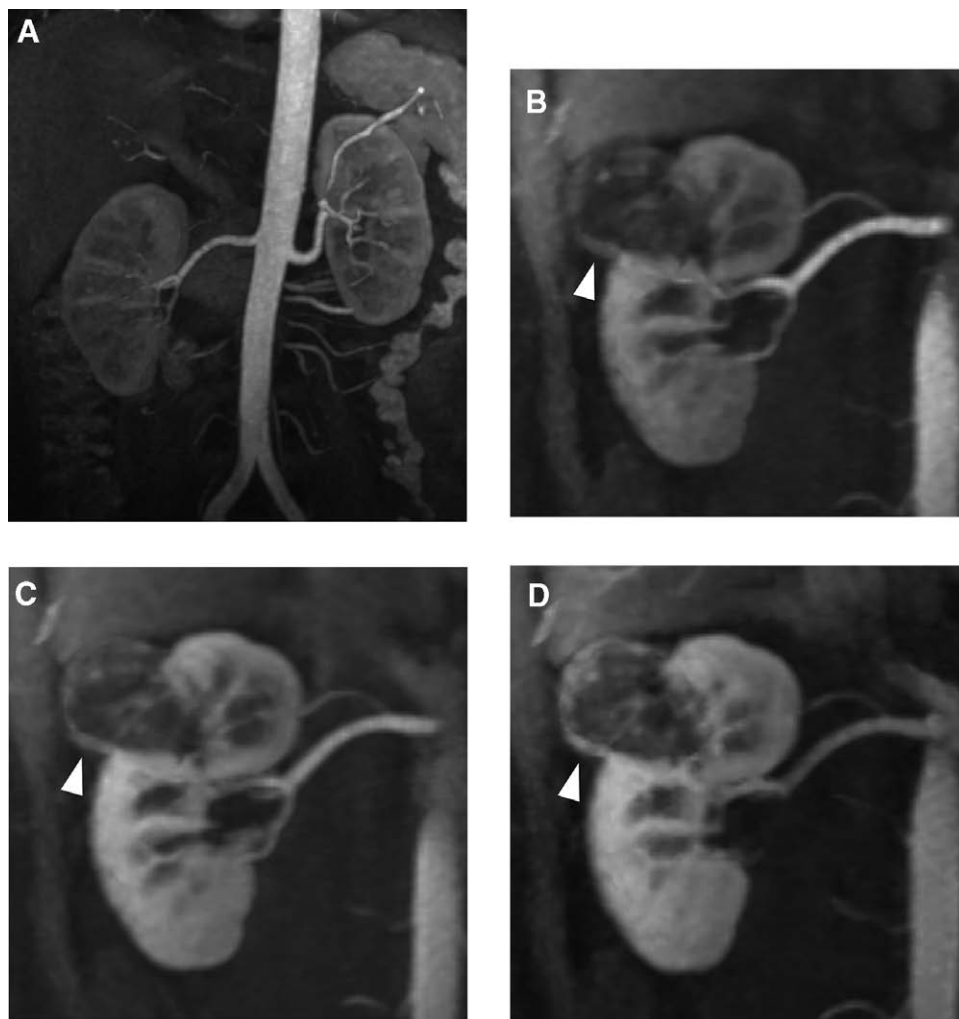

Figure 6. A 42-year-old man with angiomyolipoma in the right kidney who underwent DCE-MRI using F-DISCO with CS on MR750. (A) MIP images generated from data covering the entire region in the first phase. Renal arteries were well recognized without any overlap of renal veins. (B–D) Partial MIP images generated from the selected volumes for the left kidney in each phase. Contrast enhancement of the tumor was poor compared with the renal cortex. (B) In the first phase, (C) in the third phase, and (D) in the seventh phase. CS = compressed sensing, DCE-MRI = dynamic contrast-enhanced magnetic resonance imaging, F-DISCO = Differential subsampling with Cartesian ordering with a fat suppression pulse of spectrally selected adiabatic inversion recovery, MIP = maximum intensity projection.
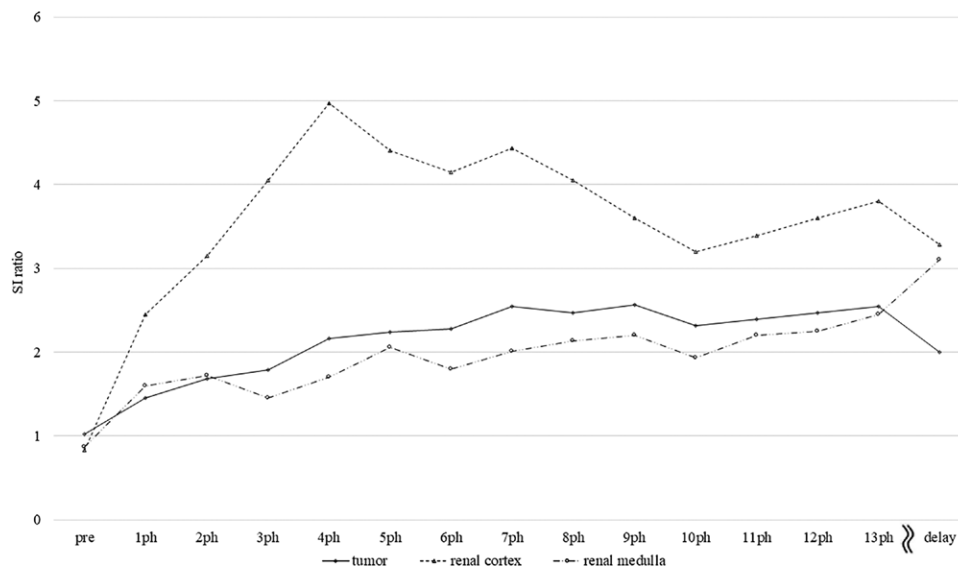
Figure 7. A 42-year-old man, same patient as in Figure 6. Time intensity curves of the right renal tumor and parenchyma after injection of contrast medium. Pre indicates initial phase after injection of contrast medium. Ph means phase. The plotted values are SI ratio calculated by dividing the SI of each ROI by the SI of the iliopsoas muscle. Pre indicates initial phase after injection of contrast medium. Delay indicates delayed phase 120 to 180 seconds after injection of contrast medium. The imaging time per phase was 1.90 seconds. ROI = regions of interest, SI = signal intensity.

recognized as an efficient fat saturation method that covers broad fat signals. However, one of the main drawbacks of this method is that it requires longer imaging times.[19] The currently used Spec IR with adiabatic pulse was optimized to minimize the prolongation of imaging time by reducing the number of modified radiofrequency pulses. Thus, acquisition times for each phase of the dynamic contrast study with F-DISCO could be set shorter than 2 seconds, even in an MR750W, a 3T magnet with a wide bore. In groups with CS, we increased the coverage of imaging because temporal resolutions are acceptable for <2 seconds per phase. The quality of fat signal suppression was found to be within acceptable levels in all the investigations we performed, which, in turn, demonstrates homogenous fat signal suppressions.

Imaging times shorter than 2 seconds with high-spatial-resolutions for each dynamic contrast phase, with an average of 1.96 seconds, have enabled us to visualize the renal arteries in all the cases without any signal overlap from the renal veins in the early dynamic phases. The presence or absence of kidney or adrenals tumors was successfully identified in all cases. One of our experimental concerns was the view-sharing features of F-DISCO, which could potentially contaminate the enhancement owing to data sharing with peripheral areas of k-space among the consecutive 4 phases. In the current study, a short imaging time that is <2 seconds for each phase may not overwhelm the loss of temporal perfusion features. In addition, contrast medium perfusions of normal anatomical structures such as renal parenchyma, medulla, and vasculatures were well recognized (Fig. 2), and data could be obtained every 2 seconds without any loss of information. Subsequently, this allowed us to characterize tissue perfusions as hypervascular or hypovascular features of the tumors. In the representative case for tumors, the contrast perfusion profile could characterize tumors, that is, early enhancement followed by the wash-out of the contrast medium (Fig. 5).

Visualization of the renal arteries without any other tissue overlap has been previously conducted in DCE-MRA, even when the temporal resolution for 1 phase was approximately 20 seconds longer by sampling the data from the center of k-space, which determines the mean contrast of the soft tissues. However, information regarding SI serial changes of the renal arteries and veins, as well as soft tissues, may be lost because

the imaging update time is not adequately short. Therefore, the currently used F-DISCO could provide us with approximately 10 high-spatial-resolution phases within a period of 20 seconds although with Dixon approach especially on a wide-bore 3, 4, or 5 phases might be obtained. Thus, dynamic contrast studies could generate SI serial changes of each structure.

We attempted to evaluate the effects of the combined use of CS to F-DISCO. Theoretically, 10% to 15% reduction in the imaging time can be accomplished for CS in current settings. Without the combined use of CS, 2 seconds imaging time for each dynamic phase could be set by using a total parallel imaging factor of 3.8. Thus, with CS, a 0.2- to 0.3-second decrease in imaging time for each phase could be achieved. Among the 51 patients included in this study, 31 patients underwent DCE-MRI using F-DISCO with CS. Temporal resolution in the groups using F-DISCO with CS was 1.93 seconds in each phase, whereas this value was increased to 2.44 seconds in the same group using F-DISCO only. Overall reduction of imaging time might be approximately 10 seconds with 20 phases. The combined use of CS with F-DISCO can successfully reduce the imaging time, and it can reduce the BH time in dynamic studies, although temporal resolution for each dynamic phase was found to be competitive between using and not using CS.

Therefore, we can apply CS to F-DISCO in clinical settings because the image quality and usability of this sequence were found to be within acceptable levels. Recent improvements in computer powers for image reconstruction have further enabled researchers to reduce the acceptable reconstruction time within several minutes for an overall dynamic contrast study.[20]

Our study suffers from several limitations. First, this study included a small number of patients with renal arteries disease or/ and renal or adrenal pathologies. As a result, the number of patient groups on MR750 or MR750W with or without CS was evidently small. Hence, in the future, we are planning to increase the number of patients involved in the experimental processes. Second, the pathological diagnosis could not be obtained in certain cases, and tumor diagnosis was conducted clinically. Third, investigations with CS were performed after the use of F-DISCO without CS. Thus, a time lag between the groups with and without CS existed.

In conclusion, dynamic contrast studies for the evaluation of renal vasculatures and tumors using F-DISCO on MR750 or MR750W with or without CS can be performed with high

temporal resolutions in a clinical 3T system. In all cases examined, selective visualization of the renal arteries and veins could be performed, and information regarding contrast media perfusion for soft tissues could be obtained. This information can be obtained in a stable fashion throughout the dynamic contrast study. CS can additionally provide benefits that the total imaging time may be shorter than without CS.

Author contributions

Study concept and design: T. Masui.

Data acquisition: T. Yamada, M. Sasaki, M. Katayama.

Data analysis and interpretation: T. Yamada, T. Masui, Y. Iwadate, N. Takei.

Data interpretation of data: T. Yamada, T. Masui, Y. Iwadate.

Drafting and manuscript revision: T. Yamada, T. Masui, Y. Iwadate, N. Takei, M. Miyoshi.

Final approval of manuscript. T. Yamada, T. Masui, Y. M. Sasaki, Iwadate, N. Takei, M. Miyoshi.

References

[1] Zhang H, Maki JH, Prince MR. 3D contrast-enhanced MR aortography. J Magn Reson Imaging. 2007;25:13–25.

[2] Kinner S, Eggebrecht H, Maderwald S, et al. Dynamic MR angiography in acute aortic dissection: 4D MRA in acute aortic dissection. J Magn Reson Imaging. 2015;42:505–14.

[3] Glockner JF, Vrtiska TJ. Renal MR and CT angiography: current concepts. Abdom Imaging. 2007;32:407–20.

[4] Sutter R, Nanz D, Lutz AM, et al. Assessment of aortoiliac and renal arteries: MR angiography with parallel acquisition versus conventional MR angiography and digital subtraction angiography. Radiology. 2007;245:276–84.

[5] Riederer SJ, Stinson EG, Weavers PT. Technical aspects of contrast-enhanced MR angiography: current status and new applications. Magn Reson Med Sci. 2018;17:3–12.

[6] Sun MRM, Ngo L, Genega EM, et al. Renal cell carcinoma: dynamic contrast-enhanced MR imaging for differentiation of tumor subtypes-correlation with pathologic findings. Radiology. 2009;250:793–802.

[7] Ho VB, Allen SF, Hood MN, et al. Renal masses: quantitative assessment of enhancement with dynamic MR imaging. Radiology. 2002;224:695–700.

[8] Hecht EM, Israel GM, Krinsky GA, et al. Renal masses: quantitative analysis of enhancement with signal intensity measurements versus qualitative analysis of enhancement with image subtraction for diagnosing malignancy at MR imaging. Radiology. 2004;232:373–8.

[9] Wei Y, Deng L, Yuan Y, et al. Gadoxetate acid disodium-enhanced MRI: Multiple arterial phases using differential sub-sampling with Cartesian ordering (DISCO) may achieve more optimal late arterial phases than the single arterial phase imaging. Magn Reson Imaging. 2019;61:116–23.

[10] Saranathan M, Rettmann DW, Hargreaves BA, et al. DIfferential sub-sampling with cartesian ordering (DISCO): a high spatio-temporal resolution Dixon imaging sequence for multiphasic contrast enhanced abdominal imaging. J Magn Reson Imaging. 2012;35:1484–92.

[11] Fritz S. Whole-body MRI at high field: technical limits and clinical potential. Eur Radiol. 2005;15:946–59.

[12] Ma J. Dixon techniques for water and fat imaging. J Magn Reson Imaging. 2008;28:543–58.

[13] Lustig M, Donoho D, Pauly JM. Sparse MRI: the application of compressed sensing for rapid MR imaging. Magn Reson Med. 2007;58:1182–95.

[14] Takei N, Wang K, Estkowski L, et al. Fat suppressed highly accelerated dynamic imaging utilizing view sharing, compressed sensing and parallel imaging. In: Proceedings of the 25th Annual Meeting of ISMRM, Honolulu, USA, April 22-27, 2017. p. 5148.

[15] King K, Xu D, Brau AC, Lai P, Beatty PJ, Marinelli L. A new combination of compressed sensing and data driven parallel imaging. In: Proceedings of the 18th Annual Meeting of ISMRM, Stockholm, Sweden, May 3-7, 2010. p. 4881.

[16] Brau AC, Beatty PJ, Skare S, et al. Comparison of reconstruction accuracy and efficiency among autocalibrating data-driven parallel imaging methods. Magn Reson Med. 2008;59:382–95.

[17] Ichikawa S, Motosugi U, Oishi N, et al. Ring-like enhancement of hepatocellular carcinoma in gadoxetic acid–enhanced multiphasic hepatic arterial phase imaging with differential subsampling with Cartesian ordering. Invest Radiol. 2018;53:191–9.

[18] Kim YC. Advanced methods in dynamic contrast enhanced arterial phase imaging of the liver. Investig Magn Reson Imaging. 2019;23:1–16.

[19] Lauenstein TC, Sharma P, Hughes T, et al. R. Evaluation of optimized inversion-recovery fat-suppression techniques for T2-weighted abdominal MR imaging. J Magn Reson Imaging. 2008;27:1448–54.

[20] Dyvorne HA, Knight-Greenfield A, Besa C, et al. Quantification of hepatic blood flow using a high-resolution phase-contrast MRI sequence with compressed sensing acceleration. AJR. 2015;204:510–8.